Hygroscopic stresses development in epoxy-metal bonded assemblies under hydrothermal conditions

Romain Grangeat, Hector Ravon, Edvan Pinto, Adiana Nascimento, Eduardo Martins Sampaio, Silvio de Barros

Hygroscopic stresses development in epoxy-metal bonded assemblies under hydrothermal conditions

Romain Grangeat[1,*], Hector Ravon[1], Edvan Pinto[2], Adiana Nascimento[3], Eduardo Martins Sampaio[4], Silvio de Barros[1,2]

[1]CESI LINEACT, Le Paquebot, 24, 44600 Saint-Nazaire, France
[2]Federal Center of Technological Education (CEFET/RJ), Rio de Janeiro, 20271-110, Brazil
[3]Departamento de Engenharias, Universidade Federal Rural do Semi-Árido, 59780-000 Caraúbas/RN, Brasil
[4]Universidade do Estado do Rio de Janeiro-UERJ, RuaBonfim, 25. Nova Friburgo, 28625-570 Rio de Janeiro, Brazil

Abstract

Epoxy-metal bonded assemblies are widely used in various industrial applications due to their mechanical efficiency and stress distribution capabilities. However, the durability of these assemblies in humid environments remains the subject of extensive research. This study focuses on the development of a numerical hygroelastic model to investigate hygroscopic stresses in a single-lap epoxy-metal bonded assembly exposed to immersion at different temperatures and durations. The model considers a Fickian sorption behavior with hygroscopic swelling and thermal expansion, enabling a detailed analysis of stress development. As input data, experimental measurements were conducted to determine the water diffusion kinetics, the thermal expansion coefficient, the hygroscopic swelling coefficient, and the evolution of the elastic modulus during aging. The impact of temperature is discussed to evaluate the effect and relevance of accelerated aging. The role of interphases, characterized by distinct diffusion properties, is also examined to assess their impact on water content distribution and stress fields. Results highlight the critical influence of water diffusion kinetics, temperature, and interphase properties on stress distribution, emphasizing localized swelling and elevated stress levels at the adhesive-substrate interface.

Keywords: bonded assembly; hydrothermal aging; hygroscopic stresses.

I) Introduction

Bonded assembly structures, particularly epoxy/metal assemblies, play a central role in numerous industrial applications due to their high mechanical performance. Bonding also enables a more uniform stress distribution compared to other joining techniques such as welding or riveting. However, epoxy adhesives, being hydrophilic polymer materials, have the ability to absorb water when exposed to humid environments. This exposure, coupled with thermal variations, can lead to internal stresses. These stresses, primarily resulting from differential hygroscopic and thermal expansion between the substrates and the adhesive, are recognized as major factors affecting their durability and structural integrity. Recent studies on hygroscopic stresses highlight the importance of understanding interactions between materials under severe environmental conditions. Le Duigou et al. (2017) [1] focused on bio-composites based on maleic anhydride-grafted polypropylene reinforced with flax fibers, demonstrating that the hygroscopic expansion of natural fibers significantly influences interfacial stresses and shear strength.

Corresponding author: rgrangeat@cesi.fr

On the same material, Péron et al. (2019) [2] combined experimental measurements of water diffusion, hygroscopic expansion, and mechanical properties to develop a hygro-mechanical model based on laminate theory and Fickian diffusion. Their results show that hygroscopic stresses induce global deformations (curvature) and can affect the durability of fiber/matrix interfaces. Youssef et al. (2009) [3] analyzed hygroscopic stresses in epoxy/carbon composite laminates, accounting for the evolution of mechanical properties related to humidity. Their work shows that integrating hygroscopic effects and their variations into models is essential for predicting stresses and improving the durability of composite systems subjected to humid environments. Zhou et al. (2019) [4] studied epoxy coatings applied to rigid substrates, such as glass or stainless steel, and showed that incorporating modified fillers (micro- or nanofillers) into the epoxy matrix reduces the risk of interfacial cracking induced by thermal and hygroscopic stresses. Similarly, Kessentini et al. (2018) [5] numerically and analytically examined multilayer bonded structures using polymer adhesives subjected to mechanical, thermal, and hygroscopic stresses. Their coupled hygro-thermo-mechanical model reveals that differences in thermal and hygroscopic expansion coefficients between adhesives and metallic or composite substrates can cause premature interface degradation. The study of hygroscopic stresses has also been the subject of investigations in epoxy-based electronic molded compounds used in electronic packaging. For instance, Kim et al. (2015) [6] studied hygroscopic and viscoelastic stresses in MEMS devices encapsulated with epoxy molding compounds subjected to humidity and thermal cycles. They developed a numerical model based on the hygroscopic and thermal properties of materials to predict deformations and risks of delamination.

Despite significant advances in understanding hygroscopic constraints in composites, biocomposites, and multilayer structures, epoxy/metal bonded joints, particularly single lap joints remain relatively understudied. While most previous research has focused on the impact of aging on mechanical strength or failure modes [7] [8] [9] [10], this study addresses a complementary and still little-explored aspect: the gradual development of internal stresses of hydrothermal origin, without external mechanical loading. These internal stresses, although not directly visible, play a crucial role in degradation phenomena, such as interfacial damage or crack initiation.

In this context, the present work aims to address this gap by developing a numerical model to analyze hygroscopic stresses generated in an epoxy/metal assembly subjected to water aging through immersion at various temperatures. By integrating precise experimental measurements of water diffusion kinetics and hygroscopic swelling coefficients, this model will enable the study of complex interactions between diffusion, swelling, and mechanical stresses, with a particular focus on the role of interphases. These efforts will open new perspectives for optimizing bonded assemblies in humid environments.

II) Materials and methods

1. Materials and samples geometry

The adhesive used in this study is Novatec Primer NVT. It is a two-component adhesive with a polyamine hardener. This adhesive can be cross-linked at room temperature. Dog-bone tensile specimens following the ASTM D638-14 standard were manufactured (**Fig. 1**) using an aluminum mold. After manufacturing, an average thickness of 3.2 mm was measured across all the specimens. These specimens were be used to perform both tensile and gravimetric tests. Works in the literature [11] [12] have shown that water diffusion kinetics can be determined using this type of geometry. Water diffusion can be considered unidirectional along the thickness.

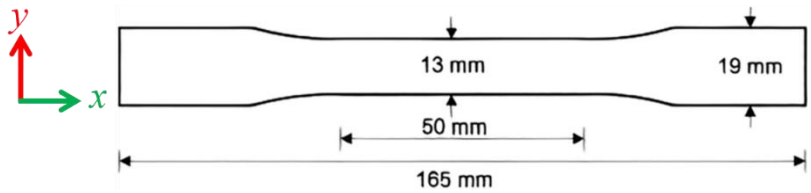

Fig. 1 - Dog-bone tensile specimens manufactured according to the ASTM D638-14 standard.

2. Gravimetric tests

Gravimetric tests were conducted to evaluate water absorption on bulk adhesive specimens immersed in water at three different temperatures: 18 °C, 40 °C, and 50 °C. These temperatures were chosen to be sufficiently far from the glass transition temperature (around 85 °C) to avoid observing a change in the material's state during aging. Specimens were initially placed in a desiccator at room temperature with an average humidity level of 17 % for two weeks. The objective was not necessarily to achieve zero water content in the specimen but rather a homogeneous water content distribution. The initial mass of specimens, m_0 was measured using an analytical balance (accuracy of 1 mg). Specimens were then immersed in thermostatic baths to ensure temperature stability. Three specimens were used for each temperature. At regular intervals, they were removed, gently wiped to remove surface water, and quickly weighed to record their mass over time, $m(t)$. This procedure was repeated until an equilibrium absorption state was reached, allowing the evaluation of water absorption kinetics by calculating the overall water content $C(t)$ of a specimen using **Eq. 1**.

$$C(t) = \frac{m(t) - m_0}{m_0} \qquad \text{(Eq. 1)}$$

In order to maintain manageable aging times, a stopping criterion was introduced for the gravimetric tests. It was agreed to stop the measurements when the variation in water uptake between two points spaced 48 hours apart became less than 0.5 %. This threshold was chosen to ensure that the sample reached a near-saturation state while optimizing the duration of the tests. This approach helps to limit excessively long experimental durations while ensuring relevant results for studying the behavior of the adhesive subjected to water absorption.

3. Thermal expansion and hygroscopic swelling measurements

A measurement bench was set up to perform precise dimensional measurements on bulk adhesive specimens (**Fig. 2**). This bench is equipped with a high-precision laser displacement sensor (Keyence LK-G82), mounted on a micrometric linear translation stage allowing movements along the *x* and *y* axes. The specimen is fixed on an adjustable table in the *z*-axis, enabling precise height positioning and ensuring optimal alignment with the sensor. This setup allows for the measurement of dimensional variations of the specimen under different exposure conditions, with sufficient precision to detect potential deformations caused by water absorption or temperature variations. Before each measurement, a reference specimen was tested to eliminate the effects of measurement bench drift.

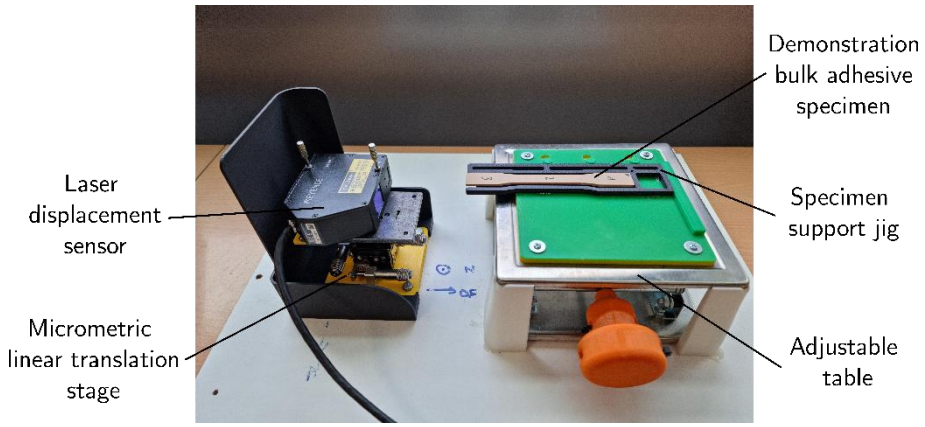

Fig. 2 - Dimensional measurement bench using a laser displacement sensor (Keyence LK-G82).

Thermal expansion measurements were carried out over a temperature range of 20 °C to 50 °C to remain consistent with the aging tests. Three specimens were placed in each oven set at 30 °C, 40 °C, and 50 °C. The specimens were left for 30 minutes to ensure homogeneous temperature distribution. They were then removed from the oven and immediately placed on the measurement bench. The dimension of each specimen was measured at a frequency of 1 Hz until stabilization at room temperature.

For hygroscopic swelling measurements, Dezulier et al. (2022) [13] demonstrated that hygroscopic swelling depends only on the material studied and not on the humidity and temperature conditions. In this context, it was decided to perform swelling measurements only for immersion aging at 50 °C.

In parallel with gravimetric measurements over time, specimens, after being removed from the 50 °C bath, were placed in a water bath at room temperature for 30 minutes. The objective was to perform measurements without being affected by thermal effects. By immersing the specimens in water, desorption effects that might occur in ambient air were minimized. After 30 minutes, the specimens were placed on the bench for dimensional measurements.

4. Hygroelastic model

The hygroelastic model enables coupling between the water uptake of the material and its mechanical properties. This model allows for the simulation of swelling effects induced by water diffusion. Initially, Fick's model, which is used to simulate water diffusion, will be presented.

In 1979, Fick developed a free-phase diffusion model based on an analogy with Fourier's model for heat conduction. Fick's model is the most widely used for water diffusion and is characterized by two parameters: D, the diffusion coefficient, representing the diffusion rate, and C_{sat}, the water content at saturation, representing the maximum amount of water the material can absorb. This law is based on the free volume theory, where water molecules exist only in a free state. Crank (1975) [14] studied numerous cases and boundary conditions by solving this problem. In a 1D case (infinite plate of thickness e), with an initially dry material and boundary conditions at C_{sat}, the solution of Fick's model in the z direction in thickness allows for determining the local water content $c(z, t)$ (**Eq. 2**) which depends on the position z in the thickness and on time t.

$$c(z,t) = C_{\text{sat}}\left(1 - \frac{4}{\pi}\sum_{n=0}^{\infty}\frac{(-1)^n}{2n+1}exp\left[-(2n+1)^2\pi^2.\frac{D.t}{e^2}\right]cos\left[(2n+1)\pi\frac{z}{e}\right]\right) \qquad \text{(Eq. 2)}$$

By integrating equation (**Eq. 2)** over the volume, the global water content $C(t)$ is given by **Eq. 3**.

$$C(t) = C_{\text{sat}}\left(1 - \frac{8}{\pi^2}\sum_{n=0}^{\infty}\frac{1}{(2n+1)^2}exp\left[-(2n+1)^2\pi^2.\frac{D.t}{e^2}\right]\right) \qquad \text{(Eq. 3)}$$

The mechanical behavior law of the hygroelastic model (**Eq. 4**) links the local hygroscopic stresses to the local water content calculated above using the solution of Fick's model.

$$\boldsymbol{\sigma}^{\mathbf{hyg}}(\mathbf{z},\mathbf{t}) = \mathbf{L}\left[\boldsymbol{\varepsilon}^{\mathbf{hyg}}(\mathbf{z},\mathbf{t}) - \mathbf{I}.\beta^{\text{hyg}}.\Delta c(z,t)\right] \qquad \text{(Eq. 4)}$$

Where $\boldsymbol{\sigma}^{\mathbf{hyg}}(\mathbf{z}, \mathbf{t})$ represents the hygroscopic stress tensor, $\mathbf{L}$ the stiffness tensor, $\boldsymbol{\varepsilon}^{\mathbf{hyg}}(\mathbf{z}, \mathbf{t})$ the hygroscopic strain tensor, $\mathbf{I}$ the identity tensor, β^{hyg} the hygroscopic swelling coefficient and $\Delta c(z, t)$ the local water content differential.

Ultimately, the resolution of this hygroelastic model is achieved by applying the fundamental principle of statics (**Eq. 5**).

$$div(\boldsymbol{\sigma}^{\mathbf{hyg}}(\mathbf{z},\mathbf{t})) = 0 \qquad \text{(Eq. 5)}$$

Subsequently, this problem is solved using finite element analysis with the Comsol software.

III) Results

The following section presents the obtained results and their analysis, based on experimental, analytical, and numerical approaches. First, kinetics of water diffusion within the bulk adhesive were studied; highlighting the impact of temperature and comparing experimental results with analytical modeling based on Fick's model and numerical simulations performed using finite element. From this work, local water content fields were determined and used as a basis for modeling water content distribution in a single-lap bonded joint. Next, the evolution of the adhesive's mechanical properties as

a function of aging was determined through tensile tests conducted in various environments and their correlation with water content. Finally, a dimensional analysis characterizes the phenomena of thermal expansion and hygroscopic swelling, before introducing a hygroelastic model illustrating hygroscopic stress fields in a single-lap bonded joint.

1. Water diffusion in bulk adhesive
    a. Experimental results and impact of temperature

Gravimetric tests were conducted during 7 months on bulk adhesive specimens following the previously explained methodology. Using **Eq. 1**, it is possible to represent the water content of specimens as a function of immersion time for three different temperatures: 18 °C, 40 °C, and 50 °C. The results are shown in **Fig. 3** as a function of the square root of time divided by the sample thickness. This unit is used to verify the linearity of the initial diffusion phase, characteristic of Fickian diffusion, and to normalize with respect to the thickness, allowing the determination of the material's behavior rather than the influence of geometry. Moreover, considering Eq. 2 and Eq. 3 dividing by the thickness allows the equation to be dimensionless. To improve the clarity of the graph and given the repeatability, it was decided to represent the average results of the three specimens for each temperature.

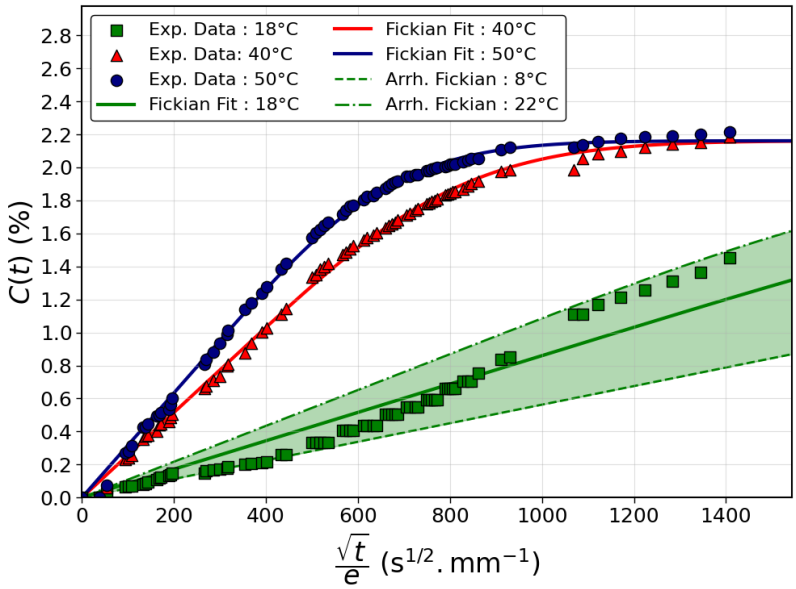

Fig. 3 - Water diffusion kinetics determined using gravimetric tests for immersion at 18 °C, 40 °C, and 50 °C.

Results presented in **Fig. 3** show that the water absorption kinetics of the epoxy adhesive following a Fickian behavior and are strongly influenced by temperature. At 50 °C, the adhesive quickly reaches a plateau corresponding to water saturation, with a maximum content of approximately 2.16 %. At 40 °C, saturation occurs more gradually but seems to approach a similar value. In contrast, at 18 °C, water absorption is significantly slower, and no plateau is reached during the test period, indicating ongoing kinetics.

Regarding the impact of temperature on the water content at saturation, studies show that this parameter mainly depends on relative humidity in polymers and composites, although it can be influenced by temperature under specific conditions. McKague et al. (1976) [15] demonstrated that water absorption is primarily governed by relative humidity, with temperature having only a limited impact on saturation. However, Vanlandingham et al. (1999) [16] observed non-Fickian behaviors at high temperatures, where microstructural modifications may influence diffusion and saturation. Similarly, Jansen et al. (2020) [17] identified a weak but non-linear relationship between saturation and relative humidity, while noting that temperature effects remain limited below 85 °C. Furthermore, several studies [18][19] report that high temperatures or prolonged exposure can lead to desorption or irreversible structural modifications, thereby indirectly affecting water absorption capacity. However, the literature does not fully agree on the dependence of water saturation on temperature. Some studies show a relationship between these two parameters, while others conclude that they are independent. A dominant trend, however, suggests that for temperatures close to the glass transition temperature (Tg), the water content at saturation is indeed influenced by temperature. In some cases, particularly for epoxy materials with high water absorption capacity [20], the decrease in glass transition temperature induced by water absorption is so significant that it approaches the aging temperature, which could explain the observed dependence of saturation on temperature.

In this study, since the aging temperatures are sufficiently distant from the glass transition temperature (around 85 °C) and the absorption kinetics appear to follow a Fickian behavior, the hypothesis of an independence of the water content at saturation with respect to temperature was retained. However, it should be kept in mind that secondary phenomena, particularly at high temperatures, could alter this behavior under specific conditions.

Initially, a least squares interpolation was performed on the experimental points at 50 °C from **Fig. 3** with the analytical solution of Fick's law (**Eq. 3**). Regarding the interpolations at 40 °C and 18 °C, based on the results from the literature, it was decided to fix the water content at saturation to 2.16 % (value obtained at 50 °C). These interpolations, shown in **Fig. 3**, demonstrate a good fit with the experimental data at 50 °C and 40 °C. Regarding the aging at 18 °C, the interpolation is of lower quality. This can be explained by the fact that the specimens were placed in a bath at room temperature without a temperature regulation system. The average temperature was initially measured at 18 °C. However, temperature variations were observed depending on the season, with around 8 °C in winter and up to 22 °C in summer. To account for these fluctuations, two additional theoretical curves were added to **Fig. 3**: one at 8 °C and one at 22 °C, based on a Fickian diffusion model with Arrhenius temperature dependence. These curves illustrate the influence of ambient temperature on the diffusion kinetics. This is a limitation of the Fick model, which does not allow for this variation in temperature during the transient phase of water uptake, so the first diffusion phase is necessarily represented linearly.

The average diffusion coefficients calculated for each temperature, along with their standard deviations, are listed in the **Tab. 1**.

Tab. 1 - Diffusion coefficients obtained by interpolating the solution of Fick's law against experimental results for different temperatures.

Temperature (°C)	D: diffusion coefficient (mm²/s)
18	3.11×10^{-8}
40	2.79×10^{-7}
50	4.22×10^{-7}

These results show the strong dependence of the diffusion rate on temperature. The literature highlights that the dependence of the diffusion coefficient on temperature follows an Arrhenius law (**Eq. 6**).

$$D(T) = D_0 . e^{-\frac{E_a}{RT}} \quad \text{(Eq. 6)}$$

Where $D(T)$ represents the coefficient diffusion in mm²/s at T temperature in K, D_0 the coefficient diffusion in mm².s^{-1} for high temperatures, R = 8.314 J.mol^{-1}.K^{-1} the gas constant and E_a the activation energy in J.mol^{-1}.

The Arrhenius law describes the exponential dependence of diffusion coefficients on temperature and is widely used to analyze water diffusion in polymers. By plotting ln(D) as a function of 1/T and performing a linear regression, it is possible to verify the validity of this law (**Fig. 4**). An activation energy of 66 kJ/mol was calculated. This value is slightly higher than those observed in the literature for polymer materials, which indicates a strong dependence on temperature. Indeed, Deroiné et al. (2014) [21] observed a linear relationship between the logarithm of water diffusion coefficients in PLA and the inverse of temperature, with an activation energy of 30 kJ/mol, while noting limitations at high temperatures due to structural change. Similarly, La Saponara et al. (2011) [22] reported Arrhenius-type behavior for diffusion in epoxy adhesives and carbon/epoxy composites, although deviations occurred in complex environments, such as hydraulic fluids. Xian et al. (2024) [23] found an activation energy of 49.14 kJ/mol for water diffusion in epoxy resins, where higher temperatures accelerated water ingress, leading to relaxation and structural degradation. Thus, the Arrhenius law provides a useful predictive framework, though deviations may occur under complex environmental conditions or in non-Fickian behaviors. Finally in their study, Zhou and Lucas (1999) [24] determined two distinct activation energies for water in epoxy resins: approximately 41.8 kJ/mol for Type I water, forming a single hydrogen bond, and 62.8 kJ/mol for Type II water, bonded through multiple hydrogen bridges. These values reflect the difference in the strength of interactions between water molecules and the polymer network. Compared to the activation energy value obtained in this work, it seems that the molecules diffuse by strongly bonded to the polymer matrix. This result could be confirmed by conducting desorption tests.

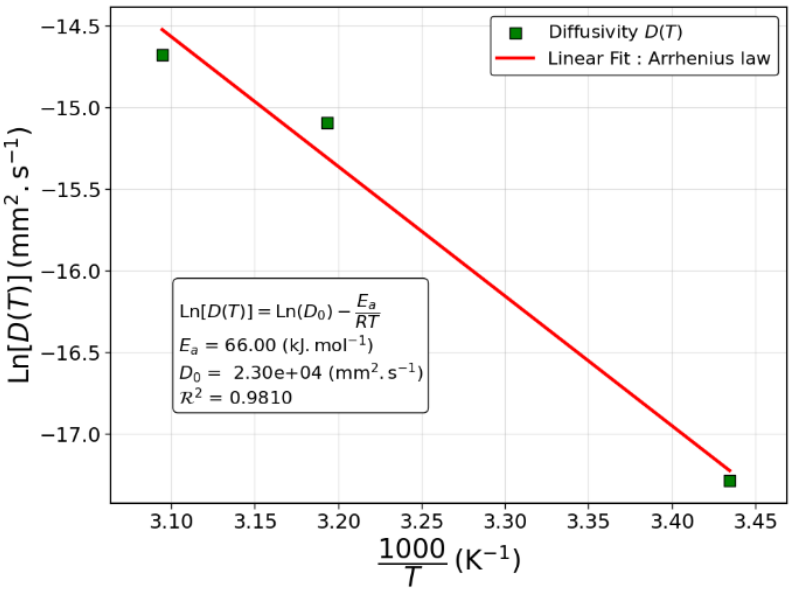

Fig. 4 - Application of the Arrhenius law and determination of the activation energy.

Using the previous results, and considering a temperature-independent water content at saturation and an activation energy of 66 kJ/mol for the diffusion coefficient, it is possible to represent the theoretic water diffusion kinetics for several temperatures between 18 °C and 50 °C (**Fig. 5**).

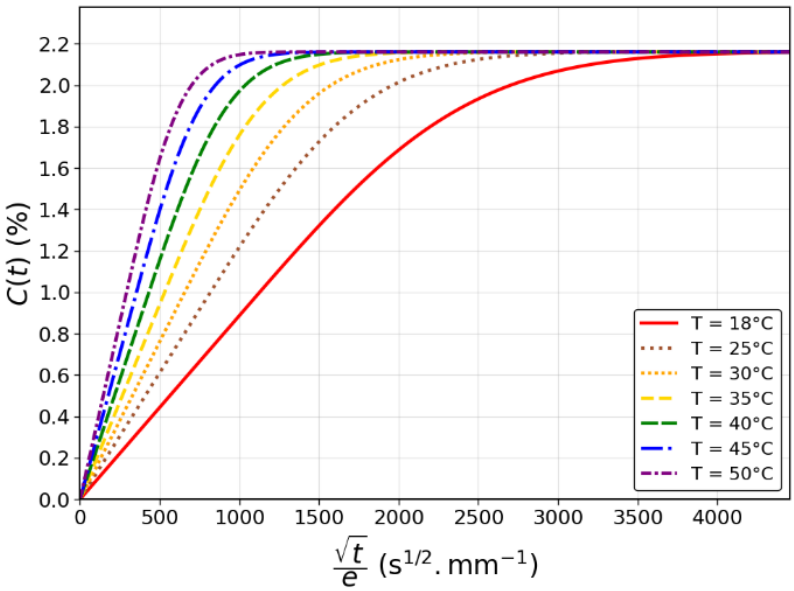

Fig. 5 - Theoretical water diffusion kinetics for different temperatures.

The representation (**Fig. 5**) allows the determination of the required saturation time and highlights the benefit of increasing the temperature to accelerate aging phenomena (while still maintaining temperatures sufficiently far from the glass transition temperature). It is still necessary, during accelerated aging, to remain sufficiently far from the glass transition temperature to avoid observing a change in the material's behavior. Saturation times can be determined and represented by considering

98 % of the water content at saturation (**Fig. 6**). The thickness considered here corresponds to the tested specimens, which is 3.2 mm.

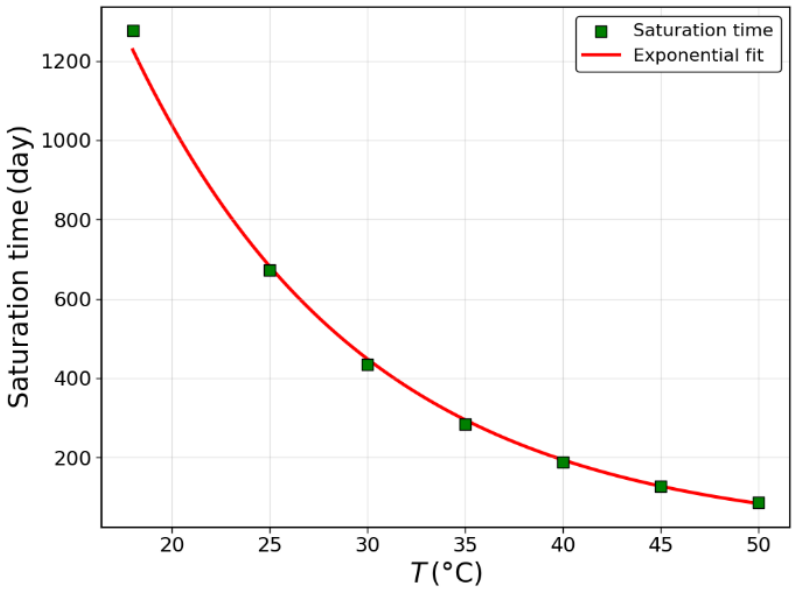

Fig. 6 - Saturation time in days as a function of aging temperature for a thickness of 3.2 mm.

According to the results in **Fig. 6**, it would take more than 1.200 days to reach saturation at 18°C, whereas saturation is achieved after 85 days of immersion at 50 °C. It is therefore essential to conduct accelerated aging tests to make experimentation times manageable within the scope of a research or industrial project. However, caution must be exercised when using an aging temperature sufficiently far from the glass transition temperature to avoid inducing a change in the material's behavior during the water diffusion process.

The experimental results and the analytical modeling based on Fick's law enabled the determination of the adhesive's diffusion coefficients at different temperatures. These coefficients are essential data for the subsequent analyses. To verify the consistency of the numerical model for its use in bonded assemblies, a finite element modeling approach is presented in the following section. This approach aims to simulate local water content fields within the adhesive and compare them with the analytical solutions (**Eq. 2)** derived from the previous results. This validation step is crucial, as the numerical model will later be used for hygroelastic modeling applied to a single-lap bonded assembly, by allowing the evaluation of hygroscopic stresses generated.

b. Numerical modeling by using finite element and water content field

To model water diffusion in the adhesive, Fick's law was used, as it accurately describes the transport of chemical species in a material based on the concentration gradient. This approach facilitates numerical implementation and allows simulation of the evolution of water content within the adhesive over time and under various boundary conditions. In the context of hygroelastic modeling, water absorption induces hygroscopic swelling, which generates deformations and mechanical stresses in the

material. This behavior is accounted for in the model by introducing a hygroscopic swelling coefficient, which links variations in water content to the resulting deformations.

To validate the diffusive part of the hygroelastic model, a simulation was performed on a rectangular specimen measuring 165 mm × 3.2 mm. The geometry was selected based on the specimens used for the gravimetric tests (**Fig. 1**), and a 1D diffusion along the *z*-axis was considered. The simulation was conducted only for water diffusion at 50 °C. The diffusion coefficient used was $D = 4.22 \times 10^{-7}$ mm²/s and the water content at saturation $C_{sat} = 2.16$ % (**Tab. 1**) corresponds to the boundary conditions imposed on the edges directly exposed to water.

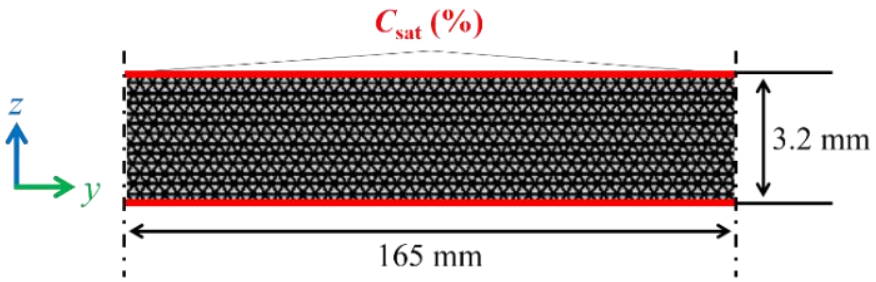

Fig. 7 - 2D Geometry, mesh, and boundary conditions used in finite element simulation of the diffusive model.

In parallel, using the local equation of the solution to Fick's model (**Eq. 2**), the water content fields were calculated analytically. The comparison between the numerical model and the analytical expression is represented (**Fig. 8**),

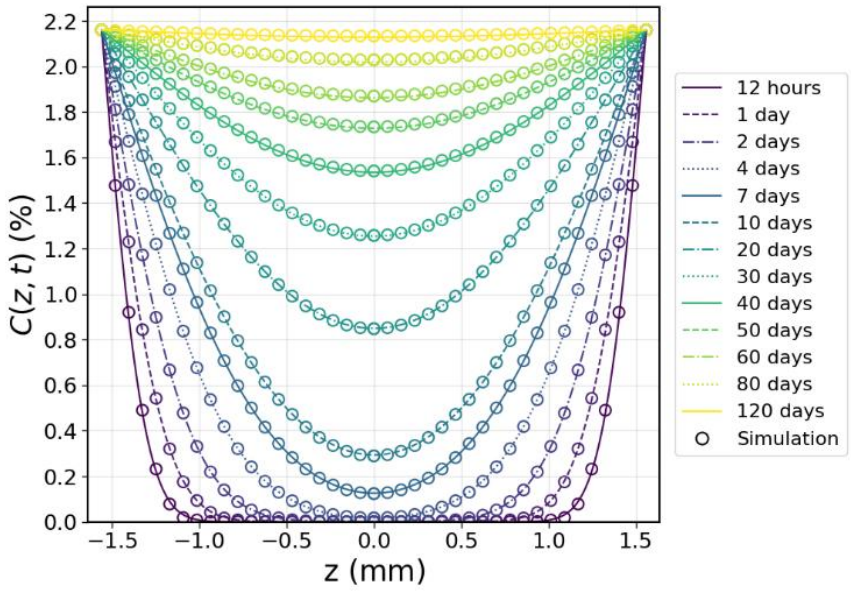

Fig. 8 - Comparison between the analytical solution (represented by lines) and the numerical model (represented by points) on local water content fields for different aging times at 50 °C.

A perfect correlation is observed between the implemented numerical model and the analytical solution regardless of the aging time considered. The numerical model can therefore be used within a bonded assembly.

2. Water diffusion in single-lap bonded joint

a. Numerical local water content field

The application of the diffusive model previously implemented for bulk adhesive allows the representation of local water content fields within a bonded assembly. It was decided to perform this modeling on a single-lap joint specimen according to the ASTM D4896 standard with orthonormal coordinate system represented in **Fig. 9**. The overlap length of the adhesive joint is 15 mm, its width is 25 mm, and its thickness is 700 µm.

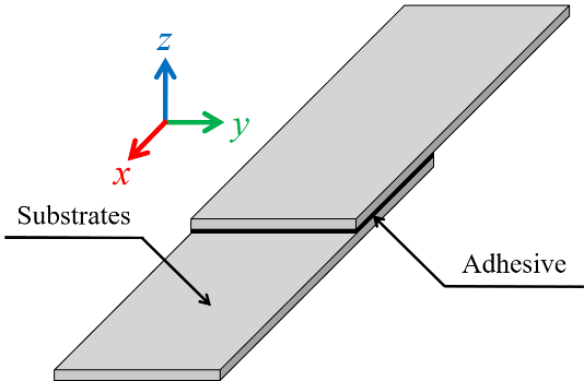

Fig. 9 - Single-lap bonded assembly (ASTM D4896).

The water uptake of the adhesive joint was modeled for three different temperatures: 18°C, 30°C, and 50°C, adhering to the diffusion coefficient value determined previously using Arrhenius's law. Cross-sectional planes were used to represent the results: the XZ plane (**Fig. 10**) positioned at the middle of the overlap width of the bonded joint, and the XY plane (**Fig. 11**) positioned at the interface between the adhesive and the upper substrate.

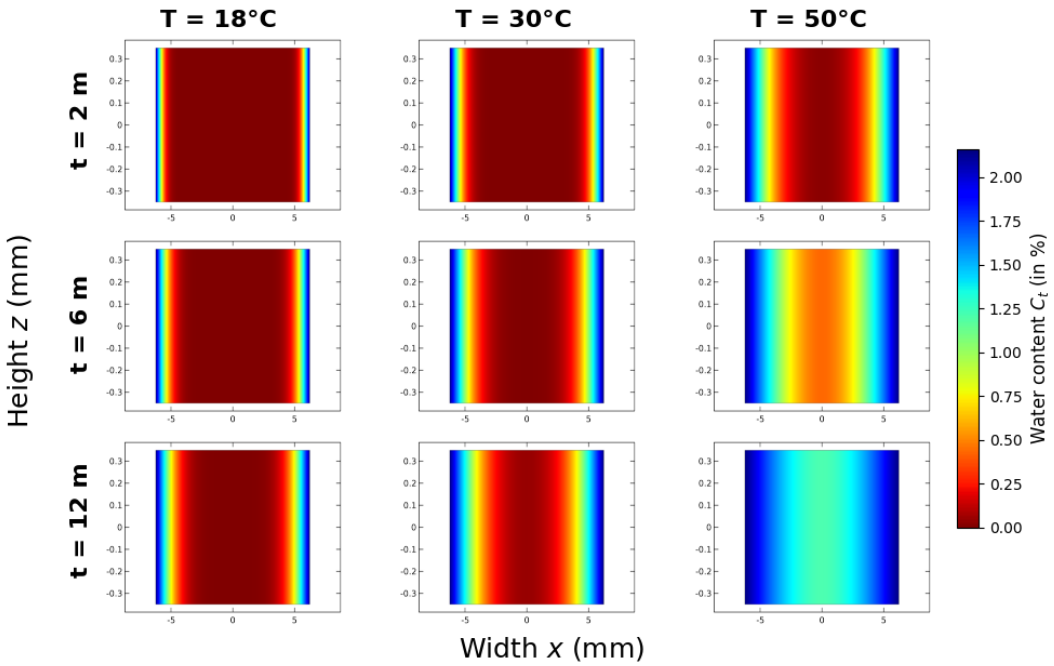

Fig. 10 - Local water content fields within a single-lap bonded assembly along the XZ plane for different time/temperature.

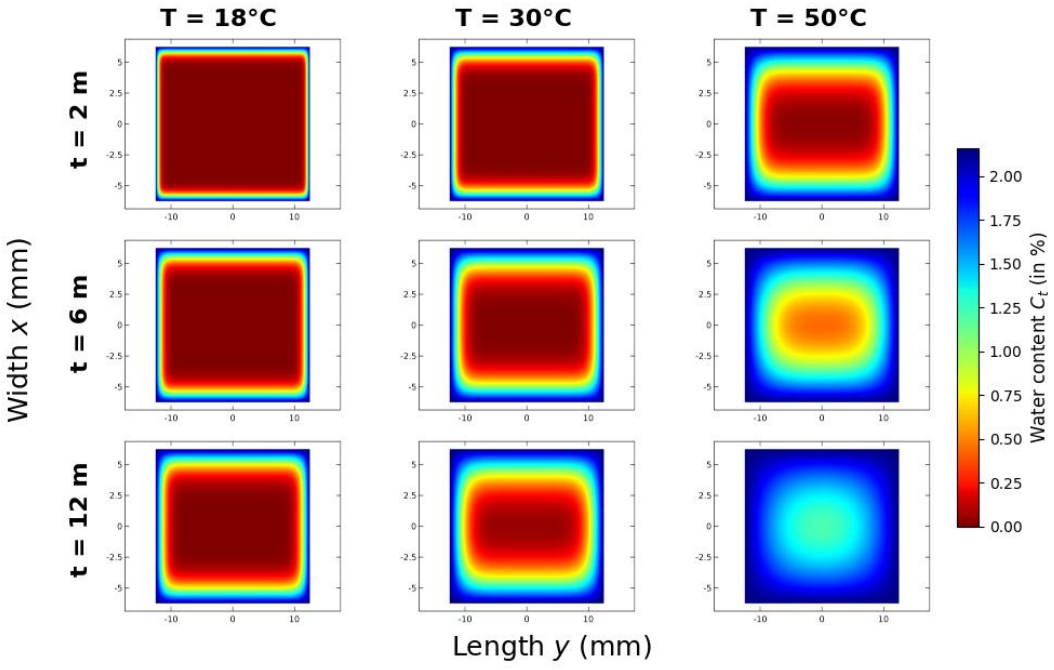

Fig. 11 - Local water content fields within a single-lap bonded assembly along the XY plane in interfacial area for different time/temperature.

In **Fig. 10** and **Fig. 11**, results showing the water content fields within a bonded joint at different temperatures and immersion times, confirm the strong dependence on temperature. After 12 months, the adhesive joint exposed to diffusion at 50 °C is quasi saturated, which is far from the case at 18 °C. **Fig.**

10 also shows a uniform diffusion front across the thickness of the adhesive joint. Based on the literature, this representation is inaccurate due to the presence of interphases, which is the subject of the next section.

b. Results and discussions on interphase's presence

Interphases, transitional zones between the adhesive and the substrate, play a critical role in water diffusion in bonded joints due to their unique physicochemical properties. This impact on water diffusion is extensively discussed in the work of Grangeat et al. (2024) [25]. which focuses on epoxy/metal bonded assemblies. Interphases promote accelerated water diffusion, attributed to a low crosslinking density and capillarity effects linked to the high surface energy of the metallic substrate, creating preferential pathways for water molecules. These mechanisms lead to localized water accumulation, amplifying swelling and hygroscopic stresses, which can weaken the assembly, alter failure modes (from cohesive to mixed or adhesive), and reduce durability. Neglecting interphases in diffusion models results in underestimating water uptake and, consequently, hygroscopic stresses, thereby compromising the prediction of assembly lifespan. Although interphases are transitional zones with property gradients, their experimental characterization is extremely challenging. They are often modeled as a finite layer with constant properties distinct from those of the bulk adhesive. Based on the review of Grangeat et al. (2024) on the impact of interphases on diffusion in epoxy/metal bonded assemblies. Based on this, the interphase in an epoxy/metal bonded assembly can be modeled as a finite layer with a thickness between 100 and 300 µm, a diffusion coefficient ten times higher than that of the bulk adhesive, and a water content at saturation 50 % greater. This approach allows for a better representation of the influence of interphases on water transport in the bonded assembly, as well as highlighting their impact on the hygroscopic stresses generated.

In this study, it was decided to set an interphase thickness of 200 µm with the following diffusive properties: $D_{\text{interphases}} = 10D_{\text{bulk}}$; $C_{\text{sat,interphases}} = 1.5C_{\text{sat,bulk}}$. By implementing the presence of these interphases, it is possible to represent the local content fields with interphases (**Fig. 12**) (**Fig. 13**) in the same way as previously (**Fig. 10**) (**Fig. 11**).

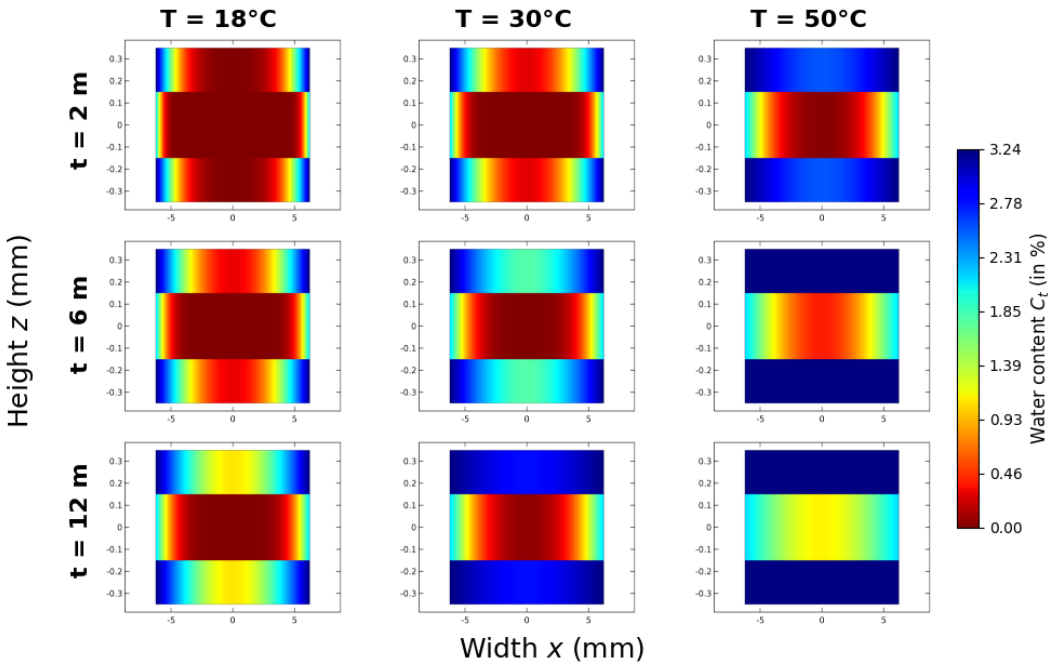

Fig. 12 - Local water content fields with interphase within a single-lap bonded assembly along the XZ plane for different time/temperature.

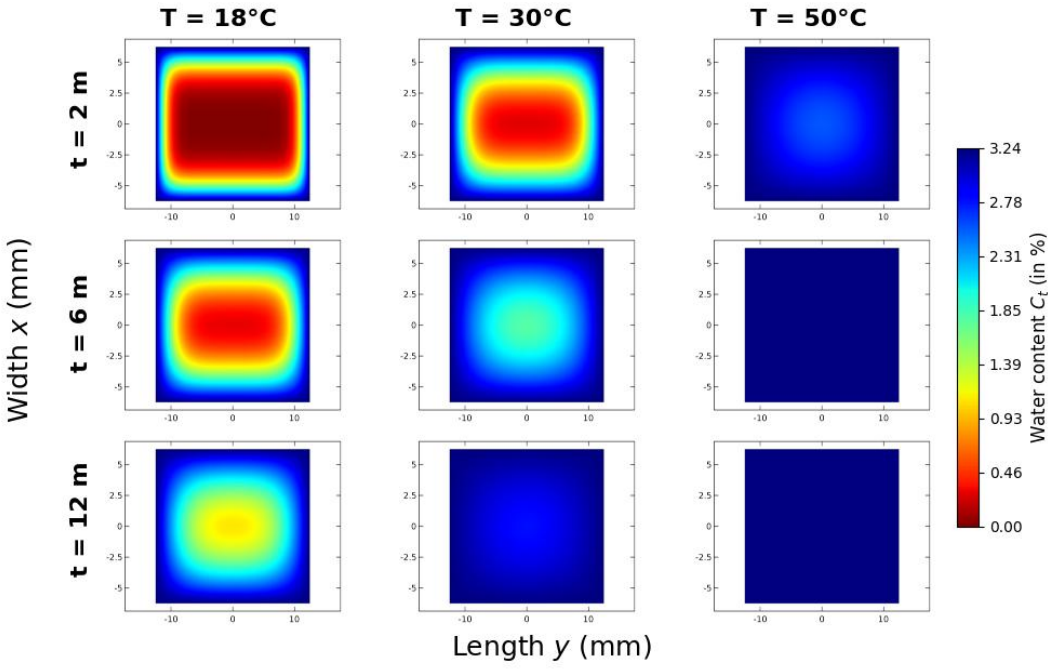

Fig. 13 - Local water content fields with interphase within a single-lap bonded assembly along the XY in interfacial area plane for different time/temperature.

First, considering the interphases results in diffusion that is ten times faster at the adhesive/substrate interface, along with a greater accumulation of water molecules, since the water content at saturation is higher. Comparing **Fig. 10** and **Fig. 12**, a change in the water diffusion front is observed, which is no

longer uniform across the thickness of the adhesive joint. The magnitude of the numerical saturation times obtained when accounting for interphases appears consistent with the literature. Indeed, Bordes et al. (2009) [20] observed changes in the fracture pattern caused by water diffusion after 3 months of immersion at room temperature. This implies that water molecules had diffused far enough to induce this change in behavior, which seems difficult to explain using the water content fields obtained without interphases after one year at 18°C (**Fig. 10**).

The model implemented here simply represents the effect of interphases by considering a finite layer, which results in a water content jump between this layer and the bulk part of the adhesive joint. In reality, it would be necessary to account for the presence of a gradient of properties, as in the work of Grangeat et al. (2023) [26]. However, the experimental approach required to establish this gradient is extremely complex and not necessarily essential in this context. Therefore, the approximation of a finite layer with constant properties appears to be a good compromise.

The numerical model implemented allows for the representation of water diffusion within a bonded joint. To better model hygroscopic stresses, it is now necessary to focus on the dependence of mechanical properties on water content. Initially, tensile tests were conducted to determine the dependence of the elastic modulus.

3. Mechanical properties during water aging

a. Experimental result: tensile tests

Tensile tests were conducted on dumbbell-shaped specimens (**Fig. 1**) in accordance with the ASTM 638-14 standard to evaluate their mechanical properties under different environmental conditions. These tests were performed using an INSTRON 3369 tensile testing machine equipped with a 50 kN load cell, allowing precise measurement of the applied forces. Specimen deformation was measured using an extensometer to ensure direct and reliable evaluation of elongation. The tests were conducted at crosshead displacement rate of 5 mm/min. To study the influence of environmental conditions, the specimens were exposed for 8 months to five different environments: in a desiccator at 18 °C (dry air), immersed in water at 18 °C, in water at 40 °C, in an oven at 50 °C (dry air), and in water at 50 °C (hot immersion). These varied conditions enabled the study of the effects of thermal and hydrolytic aging on the mechanical behavior of the tested materials. Since the objective of the work is to model hygroscopic stresses, the tensile tests were used to determine the elastic modulus of the adhesive under study. For each condition, three specimens were tested, and the elastic moduli presented below represent the average and standard deviation of the three specimens. The elastic modulus was determined within 0 to 0.25% strain as per ASTM D638-14.

Initially, an elastic modulus of 5208 ± 125 MPa was measured for the specimens that had remained in a desiccator at 18 °C for 8 months (equivalent values to the supplier data). An increase in the modulus of 5.8 % (5512 ± 39 MPa) was observed for the specimens kept in an oven at 50 °C. This increase can be explained by post-crosslinking, which occurs when sufficient energy is provided to enhance

molecular mobility and allow certain epoxy molecules to react with some molecules of the amine hardener.

For the specimens aged under immersion conditions, it is possible to represent the evolution of the elastic modulus as a function of the overall water content of the specimens. For reference, this water content is shown in **Fig. 14**. The results are discussed in the following section.

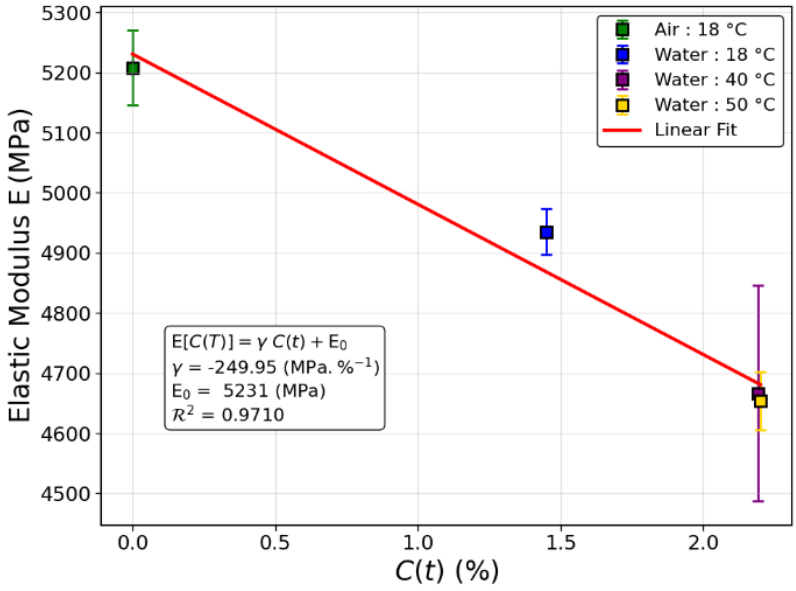

Fig. 14 - Evolution of the elastic modulus as a function of water content under different environmental conditions.

b. Discussions on water diffusion impact

The results obtained show a linear decrease in the elastic modulus as a function of the overall water content, with an estimated drop of 250 MPa per percentage of absorbed water content. For tests conducted at 18 °C in water, specimens that did not reach saturation exhibit a smaller decrease in modulus than those exposed to higher temperatures. However, it is noteworthy that the reduction in elastic modulus observed at 40 °C and 50 °C is similar. These observations suggest that the aging temperature does not have a direct impact on the degradation of the elastic modulus; only the amount of absorbed water plays a determining role. This result corroborates previous discussions indicating that, within the range of temperatures studied, the saturated water content remains independent of the aging temperature. Thus, accelerated aging at higher temperatures only serves to speed up the water uptake of materials without causing additional thermal degradation.

It is now essential to focus on the phenomenon of hygroscopic swelling of the epoxy adhesive, which induces hygroscopic stresses within a bonded assembly.

4. Dimensional measurements

a. Thermal expansion

Thermal expansion measurements were carried out on three samples at three specific temperatures: 30 °C, 40 °C, and 50 °C. These temperatures were chosen to cover the aging temperature range selected for this study. The measurements were performed using a laser displacement sensor (**Fig. 2**), ensuring high precision in capturing dimensional variations. The experimental approach is described in the "Materials and Methods" section.

The results obtained allow the evaluation of the thermal expansion coefficient α^{th} by analyzing dimensional changes as a function of temperature increase. The data show a linear evolution of thermal expansion with temperature. These results were integrated into the hygroelastic model to account for stress creation resulting from thermal expansion differences between the metallic substrates and the epoxy adhesive.

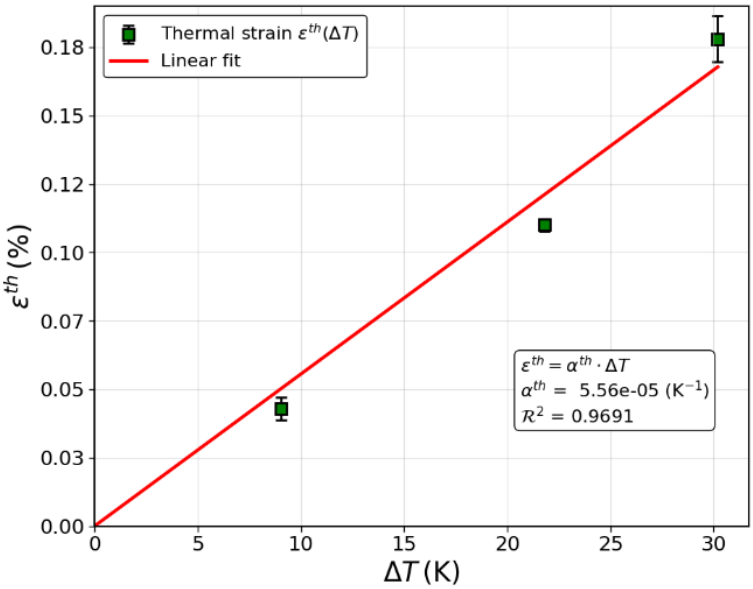

Fig. 15 - Measurement of thermal strains for the determination of the thermal expansion coefficient α^{th}.

b. Hygroscopic swelling

Hygroscopic swelling measurements were carried out during an immersion aging process at 50 °C. This temperature was chosen to accelerate the phenomenon of water diffusion. The measurements were performed using a laser displacement sensor (**Fig. 2**) on three specimens, the experimental procedure is detailed in the "Materials and Methods" section. It should be noted that the standard deviation on the measurements is 2.7 % on average.

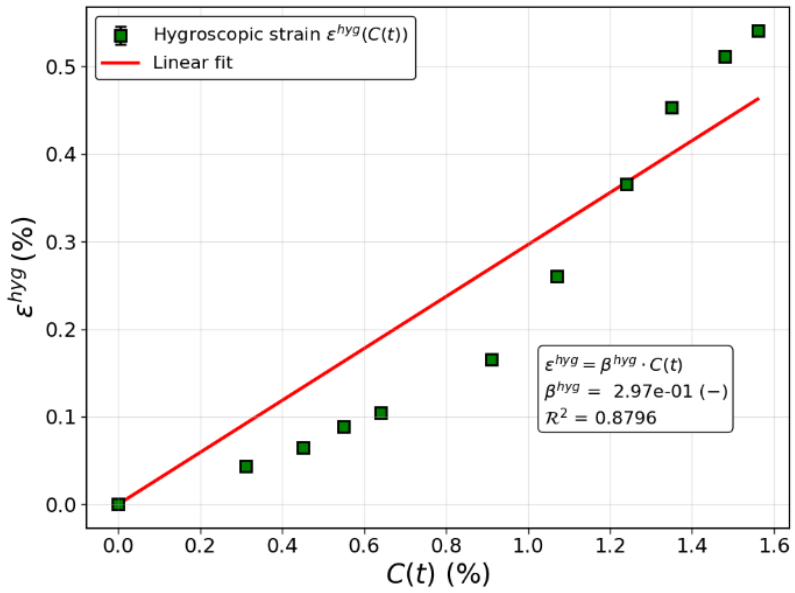

Fig. 16 - Measurement of hygroscopic strains for the determination of the hygroscopic swelling coefficient β^{hyg}.

Hygroscopic swelling measurements revealed a non-linear increase in deformations as a function of water content (**Fig. 16**), reflecting the complexity of the interactions between absorbed water and the material's structure. However, to facilitate the interpretation of the results and their integration into the hygroelastic model, it was decided to use a simplified approach based on a linear model. This approximation allows the definition of a constant hygroscopic swelling coefficient β^{hyg}, thus simplifying calculations and analysis. It would have been relevant to use a coefficient dependent on water content, as proposed in Obeid et al. (2018) [27] work's, to better represent the swelling mechanism. Nevertheless, this approach, while offering a more accurate description, significantly complicates the interpretation and use of the results in the context of this study. The choice of a linear model is therefore an acceptable compromise to achieve the objectives while maintaining an accessible and exploitable methodology.

5. Hygroscopic stresses development in single-lap bonded joint

a. Hygroscopic stresses development under hydrothermal environment

A hygroelastic model was developed for a bonded assembly whose geometry is described in **Fig. 9**. This model employs a Fickian behavior identical to that used to determine the water content fields (**Fig. 10**). The thermal expansion of the adhesive joint was incorporated into the model by accounting for the thermal expansion coefficient α^{th} measured from the results presented in **Fig. 15**. Furthermore, the hygroscopic swelling of the adhesive joint was considered using the swelling coefficient β^{hyg} obtained from the data in **Fig. 16**. The modeled mechanical stress fields include the combined contributions of stresses related to thermal expansion σ^{th} and differential hygroscopic swelling σ^{hyg} between the metallic substrates and the epoxy adhesive. Particular attention was paid to the stresses at the epoxy/substrate interface, corresponding to the XY plane. Finally, the trace of the stress tensor was represented to evaluate the overall mechanical state of the interface.

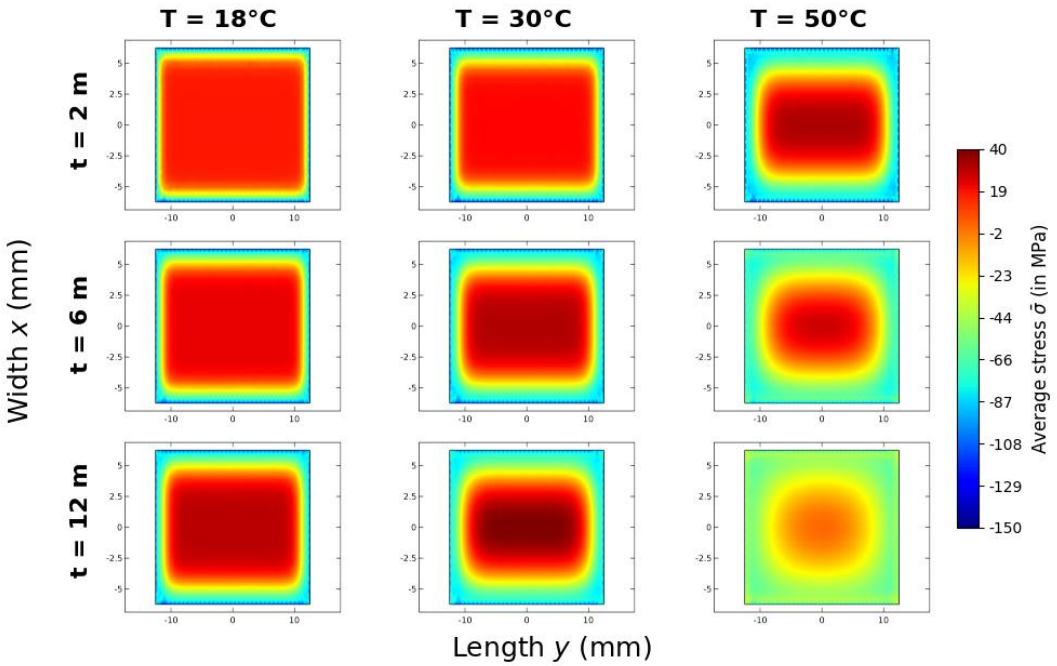

Fig. 17 – Trace of the stress tensor within a single-lap bonded assembly along the XY in interfacial area plane for different time/temperature.

Fig. 17 illustrates the evolution of the average stress (in MPa) in a bonded joint subjected to various hydrothermal aging conditions, combining immersion times (2, 6, and 12 months) and temperatures (18 °C, 30 °C, and 50 °C). The stresses shown result from two main contributions: the thermal expansion of the adhesive and the hygroscopic swelling induced by water absorption, both constrained by the substrates. In the steady state (long durations), the temperature field within the joint is assumed to be homogeneous, generating a uniform thermal stress that adds to the stresses caused by water diffusion. At the early stages of aging (t = 2 months), water begins to diffuse from the edges of the joint. This localized absorption causes swelling of the adhesive, which is restrained by the substrates, thereby generating compressive stresses at the periphery. To ensure mechanical equilibrium, tensile stresses are induced at the center of the adhesive joint, which remains dry. This behavior is observed at all temperatures but is particularly pronounced at 18 °C, where diffusion is slower. However, it should be noted that the very high stress levels at the joint edges are amplified by the boundary conditions of the numerical model and are not representative of the actual physical behavior. As temperature increases, water diffusion accelerates, leading to a faster redistribution of stresses within the adhesive. At 30 °C, a gradual homogenization of the stress field is observed by 6 months. At 50 °C, this homogenization is nearly reached by 6 months, indicating a state close to water saturation. In this condition, internal stresses tend to stabilize around -30 MPa. The thermal component, homogeneous at this temperature and estimated at approximately -10 MPa, indicates that the remaining stress results from hygroscopic swelling.

b. Results and discussions on interphase's presence

In the same way as previously during the calculation of water content fields (**Fig. 13**), the interphases were taken into account in the hygroelastic model. The stress calculation was performed using the same methodology as that used for **Fig. 17**, considering the trace of the stress tensor. This allows for an assessment of the effects of interphases on the mechanical state of the structure.

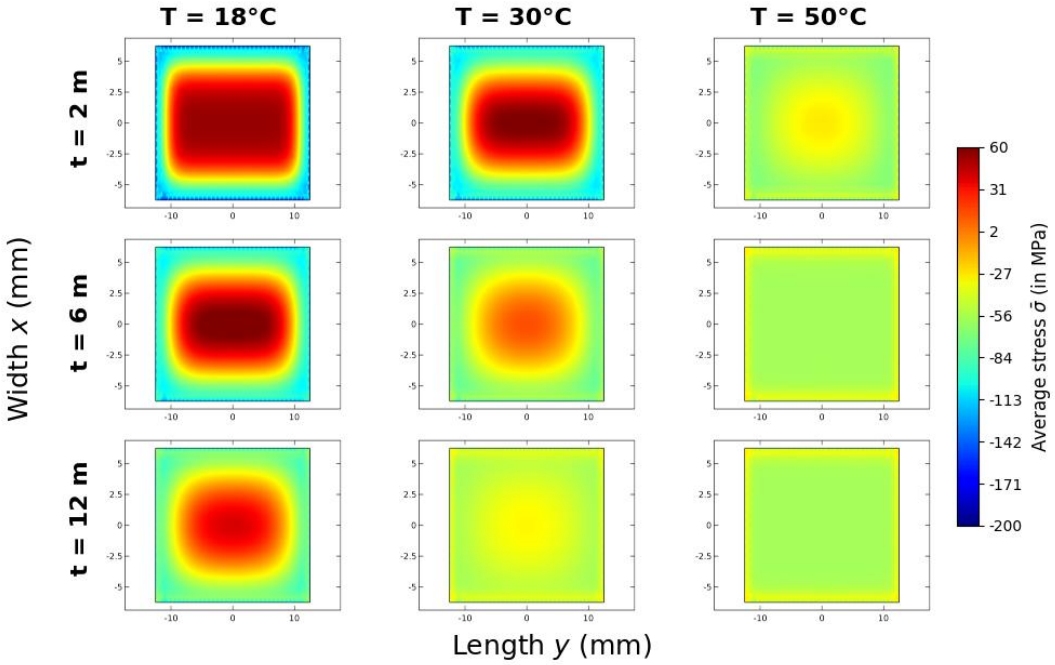

Fig. 18 - Trace of the stress tensor with interphases within a single-lap bonded assembly along the XY in interfacial area plane for different time/temperature.

By comparing the results of **Fig. 17** and **Fig. 18**, accounting for the interphases leads to much faster water saturation and, consequently, a stress field that homogenizes more quickly. However, since the water content at saturation is higher, the mechanical state of the adhesive joint tends towards a homogeneous compressive stress field that is higher than when the interphases are not considered. Indeed, the stress field tends toward a compressive stress of -30 MPa without the interphases, compared to -46 MPa with the interphases. It is important to note, however, that the stresses observed in the case with interphases are strongly influenced by the mechanical and diffusion properties attributed to these areas. In this study, these properties were not specifically characterized for the epoxy used, but rather taken from literature data, potentially obtained from different formulations. As a result, the findings related to interphase modeling should be regarded with caution and considered more indicative than quantitatively conclusive.

IV) Conclusion

This study allowed for a deeper understanding of hygroscopic constraints in epoxy-metal bonded assemblies subjected to hydrothermal conditions. Experimental measurements showed that water diffusion in the epoxy adhesive follows Fickian behavior, regardless of immersion temperature. Through interpolation, it was possible to determine the diffusion coefficient and water content at saturation, the latter being independent of temperature. The results confirm that the effect of temperature is limited to accelerating diffusion kinetics, as highlighted by the Arrhenius relationship applied to the diffusion coefficient, with an activation energy measured at 66 kJ/mol.

A water model was developed to represent water content fields in a single-lap bonded assembly. This model, validated through comparison with analytical solutions, reveals a strong dependence of diffusion gradients on the presence of interphases. By incorporating interphase properties derived from the literature, such as a diffusion coefficient ten times higher and a water content at saturation 50% greater, the model demonstrates localized water accumulation at interfaces, significantly altering the distribution of water content fields.

Experimental measurements of thermal expansion, hygroscopic swelling, and elastic modulus provided the necessary input data for the hygroelastic model. This model enabled the simulation of stress fields generated by thermal expansion and differential hygroscopic swelling between the adhesive and metallic substrates. The results reveal that localized stresses are primarily compressive at the interfaces due to constrained hygroscopic swelling, with fields tending to homogenize over time (around -43 MPa). The inclusion of interphases in the model accentuates these effects, leading to faster saturation and higher compressive stress fields (around -56 MPa).

The results of this study highlight the importance of diffusion properties and interphases in modeling hygroscopic constraints. The methodology combining experiments and modeling provides valuable tools for predicting the long-term performance of bonded assemblies exposed to humid environments, as the resulting stress fields could explain the change in fracture patterns commonly observed during wet aging of bonded assemblies.

It is important to note that in this study, a zero stress field was assumed before exposure to hydrothermal conditions. However, this assumption does not account for the initial stresses generated during adhesive application. Indeed, the differential shrinkage of the adhesive during its curing reaction is constrained by the metallic substrates, generating residual stresses in the bonded joint. These initial stresses can be significant and influence the properties of the bonded joint. It might be interesting to exploit the water diffusion properties in the adhesive to mitigate these residual stresses. In fact, water absorption by the adhesive induces hygroscopic swelling that could partially offset the adhesive's initial shrinkage. This approach could be explored as a potential way to mitigate residual internal stresses and enhance long-term durability of bonded assemblies. A more comprehensive model integrating these initial stresses and their interaction with diffusion and swelling phenomena would refine predictions of stress fields and optimize implementation and aging protocols.

Acknowledgment

The author, Romain Grangeat, thanks the Pays de la Loire Region for its financial support as part of the PULSAR Academy. This funding has been essential for the completion of this work.

Bibliography

[1] A. Le Duigou, J. Merotte, A. Bourmaud, P. Davies, K. Belhouli, et C. Baley, « Hygroscopic expansion: A key point to describe natural fibre/polymer matrix interface bond strength », *Composites Science and Technology*, vol. 151, p. 228-233, oct. 2017, doi: 10.1016/j.compscitech.2017.08.028.

[2] M. Péron, A. Célino, M. Castro, F. Jacquemin, et A. Le Duigou, « Study of hygroscopic stresses in asymmetric biocomposite laminates », *Composites Science and Technology*, vol. 169, p. 7-15, janv. 2019, doi: 10.1016/j.compscitech.2018.10.027.

[3] G. Youssef, S. Fréour, et F. Jacquemin, « Effects of moisture-dependent properties of constituents on the hygroscopic stresses in composite structures », *Mech Compos Mater*, vol. 45, nº 4, p. 369-380, juill. 2009, doi: 10.1007/s11029-009-9098-1.

[4] H. Zhou, H.-Y. Liu, K. Fu, H. Yuan, X. Du, et Y.-W. Mai, « Numerical Simulation of Failure of Composite Coatings due to Thermal and Hygroscopic Stresses », *Coatings*, vol. 9, nº 4, p. 243, avr. 2019, doi: 10.3390/coatings9040243.

[5] R. Kessentini, O. Klinkova, H. Jrad, I. Tawfiq, et M. Haddar, « Analytical and numerical investigation of coupled hygro-thermo-mechanical model of multi-layers bonded structure », *International Journal of Adhesion and Adhesives*, vol. 84, p. 108-118, août 2018, doi: 10.1016/j.ijadhadh.2018.02.031.

[6] Y. Kim, D. Liu, H. Lee, R. Liu, D. Sengupta, et S. Park, « Investigation of Stress in MEMS Sensor Device Due to Hygroscopic and Viscoelastic Behavior of Molding Compound », *IEEE Trans. Compon., Packag. Manufact. Technol.*, vol. 5, nº 7, p. 945-955, juill. 2015, doi: 10.1109/TCPMT.2015.2442751.

[7] S. Sugiman, A. D. Crocombe, et I. A. Aschroft, « The fatigue response of environmentally degraded adhesively bonded aluminium structures », *International Journal of Adhesion and Adhesives*, vol. 41, p. 80-91, mars 2013, doi: 10.1016/j.ijadhadh.2012.10.003.

[8] S. Sugiman et A. D. Crocombe, « The static and fatigue responses of aged metal laminate doublers joints under tension loading », *Journal of Adhesion Science and Technology*, vol. 30, nº 3, p. 313-327, févr. 2016, doi: 10.1080/01694243.2015.1104079.

[9] S. Sugiman, A. D. Crocombe, et I. A. Aschroft, « Experimental and numerical investigation of the static response of environmentally aged adhesively bonded joints », *International Journal of Adhesion and Adhesives*, vol. 40, p. 224-237, janv. 2013, doi: 10.1016/j.ijadhadh.2012.08.007.

[10] X. Han, A. D. Crocombe, S. N. R. Anwar, et P. Hu, « The strength prediction of adhesive single lap joints exposed to long term loading in a hostile environment », *International Journal of Adhesion and Adhesives*, vol. 55, p. 1-11, déc. 2014, doi: 10.1016/j.ijadhadh.2014.06.013.

[11] A. Boisseau, P. Davies, et F. Thiebaud, « Sea Water Ageing of Composites for Ocean Energy Conversion Systems: Influence of Glass Fibre Type on Static Behaviour », *Appl Compos Mater*, vol. 19, nº 3-4, p. 459-473, juin 2012, doi: 10.1007/s10443-011-9219-6.

[12] M. D. Banea, L. F. m. D. Silva, R. Carbas, et S. D. Barros, « Effect of Temperature and Moisture on the Tensile Properties of a TEPs-Modified Adhesive », *Mat.Plast.*, vol. 55, nº 4, p. 478-481, déc. 2018, doi: 10.37358/MP.18.4.5057.

[13] Q. Dezulier, A. Clement, P. Davies, M. Arhant, B. Flageul, et F. Jacquemin, « Water ageing effects on the elastic and viscoelastic behaviour of epoxy-based materials used in marine environment », *Composites Part B: Engineering*, vol. 242, p. 110090, août 2022, doi: 10.1016/j.compositesb.2022.110090.

[14] J. Crank, *The mathematics of diffusion*, 2d ed. Oxford, [Eng]: Clarendon Press, 1975.

[15] McKague, L., Reynolds, J.D., et Halkias, J.E., « Moisture diffusion in fiber reinforced plastics », *Journal of engineering materials and technology*, 1976.

[16] M. R. Vanlandingham, R. F. Eduljee, et J. W. Gillespie, « Moisture diffusion in epoxy systems », *J. Appl. Polym. Sci.*, vol. 71, nº 5, p. 787-798, janv. 1999, doi: 10.1002/(SICI)1097-4628(19990131)71:5<787::AID-APP12>3.0.CO;2-A.

[17] K. M. B. Jansen, M. F. Zhang, L. J. Ernst, D.-K. Vu, et L. Weiss, « Effect of temperature and humidity on moisture diffusion in an epoxy moulding compound material », *Microelectronics Reliability*, vol. 107, p. 113596, avr. 2020, doi: 10.1016/j.microrel.2020.113596.

[18] X. Fan et V. Nagaraj, « In-situ moisture desorption characterization of epoxy mold compound », in *2012 13th International Thermal, Mechanical and Multi-Physics Simulation and Experiments in Microelectronics and Microsystems*, Cascais, Portugal: IEEE, avr. 2012, p. 1/6-6/6. doi: 10.1109/ESimE.2012.6191772.
[19] Bao et Lee, « Effect of temperature on moisture absorption in a bismaleimide resin and its carbon ®ber composites », 2002.
[20] M. Bordes, P. Davies, J.-Y. Cognard, L. Sohier, V. Sauvant-Moynot, et J. Galy, « Prediction of long term strength of adhesively bonded steel/epoxy joints in sea water », *International Journal of Adhesion and Adhesives*, vol. 29, nº 6, p. 595-608, sept. 2009, doi: 10.1016/j.ijadhadh.2009.02.013.
[21] M. Deroiné *et al.*, « Accelerated ageing of polylactide in aqueous environments: Comparative study between distilled water and seawater », *Polymer Degradation and Stability*, vol. 108, p. 319-329, oct. 2014, doi: 10.1016/j.polymdegradstab.2014.01.020.
[22] V. La Saponara, « Environmental and chemical degradation of carbon/epoxy and structural adhesive for aerospace applications: Fickian and anomalous diffusion, Arrhenius kinetics », *Composite Structures*, vol. 93, nº 9, p. 2180-2195, août 2011, doi: 10.1016/j.compstruct.2011.03.005.
[23] G. Xian *et al.*, « Water absorption and property evolution of epoxy resin under hygrothermal environment », *Journal of Materials Research and Technology*, vol. 31, p. 3982-3997, juill. 2024, doi: 10.1016/j.jmrt.2024.07.123.
[24] J. Zhou et J. P. Lucas, « Hygrothermal effects of epoxy resin. Part I: the nature of water in epoxy », *Polymer*, vol. 40, nº 20, p. 5505-5512, sept. 1999, doi: 10.1016/S0032-3861(98)00790-3.
[25] R. Grangeat, M. Girard, S. De Barros, et F. Jacquemin, « An overview of interphase's formation and participation on water diffusion in epoxy/metal bonded assemblies », *The Journal of Adhesion*, vol. 100, nº 3, p. 157-177, févr. 2024, doi: 10.1080/00218464.2023.2206960.
[26] R. Grangeat, M. Girard, C. Lupi, et F. Jacquemin, « Local water content field within an epoxy/metal bonded assembly in immersion », *The Journal of Adhesion*, vol. 99, nº 3, p. 432-448, févr. 2023, doi: 10.1080/00218464.2021.2021893.
[27] H. Obeid, A. Clément, S. Fréour, F. Jacquemin, et P. Casari, « On the identification of the coefficient of moisture expansion of polyamide-6: Accounting differential swelling strains and plasticization », *Mechanics of Materials*, vol. 118, p. 1-10, mars 2018, doi: 10.1016/j.mechmat.2017.12.002.